Magic Islands and Submonolayer Scaling in Molecular Beam Epitaxy

Michael Schroeder and Dietrich E. Wolf*
Theoretische Physik, FB 10, Gerhard Mercator Universität, 47048 Duisburg, Germany
(Received 5 August 1994)

The characteristic distance l between nucleation sites and the island size distribution are studied for layer-by-layer growth. A derivation is given that the scaling of l with the deposition rate depends only on the size of the smallest stable rather than the largest unstable island. This is important if larger islands are less stable than smaller ("magic") ones. A new algorithm for simulating molecular beam epitaxy is used to verify this result. It is shown that the size distribution function scales with the average island size only if magic islands are absent. Finite size effects for the density of stable islands and of adatoms are studied and related to the transition to step flow growth on vicinal surfaces.

PACS numbers: 68.35.Fx, 61.43.Hv, 68.55.–a, 82.20.Mj

The growth of thin films by molecular beam epitaxy (MBE) has attracted increasing attention over the last decade due to its technical importance, but also because it provides a particularly clean example of nonequilibrium surface science. The refinement of surface sensitive experimental techniques like scanning tunneling microscopy (STM) or diffraction methods has provided powerful tools for comparing theoretical predictions and experimental results. In particular, research on growth which proceeds atomic layer by atomic layer has made it possible to deduce microscopic quantities, such as binding energies, critical cluster sizes, and diffusion constants from "macroscopic" ones like island size distributions [1] and typical length scales on the surface [2,3].

One of the classical results [4,5] for the nucleation of two-dimensional islands in layer-by-layer growth is that the characteristic distance l between nucleation sites has a power law dependence on the ratio between the surface diffusion constant D and the deposition rate F:

$$l \sim \left(\frac{D}{F}\right)^{\gamma}. \tag{1}$$

This length can be measured, e.g., by determining the density of stable islands l^{-2} with STM [2]. More specifically one can measure the densities $\rho_s(\theta, D/F)$ of islands of size s [1]. Bartelt and Evans [6] discovered that the coverage θ and D/F enter the normalized distribution $s\rho_s/\theta$ only through the average cluster size $\bar{s}(\theta, D/F)$:

$$\rho_s = \frac{\theta}{\bar{s}^2} f\left(\frac{s}{\bar{s}}\right) \quad \text{with } \bar{s} = \sum_s s^2 \rho_s/\theta\,. \tag{2}$$

This has been confirmed experimentally [1]. Recently it has also been demonstrated [7,8] that the edge diffusion responsible for getting fractal or compact islands does not change the scaling function f.

The main result presented here is that (2) is not valid if the smallest stable cluster, whose size determines γ, is a magic island [9], i.e., if it is stable while larger islands are unstable. Therefore the size distribution function gives independent information on the s dependence of binding energies, which cannot be obtained from measuring the characteristic length (1). We also present the first systematic study of finite size effects of MBE simulations.

Equation (1) can be derived from a simple estimate of the nucleation rate [10,11]. Consider the time evolution starting from a flat substrate without islands. As the coverage increases the distance between island centers decreases until it locks into a minimal value l, when islands start to interact. This happens when the area l^2 is spanned by an island which contains $\sim(l/a)^{d_f}$ atoms, where d_f is its fractal dimension and a is the lattice constant. Hence the duration of the nucleation period is given by $FT_{\text{nuc}}l^2 = (l/a)^{d_f}$. As there is one nucleation event per area l^2 during T_{nuc}, the nucleation rate can be estimated by $(l^2 T_{\text{nuc}})^{-1} = F(a/l)^{d_f}$.

An independent expression for the nucleation rate can be derived from rate equations so that one obtains an implicit equation for l:

$$\left(\frac{a}{l}\right)^{d_f} \approx l^4 \frac{F}{D} \prod_{s=2}^{i^*} \frac{p_s(l)}{q_s(l)}, \tag{3}$$

with

$$p_s = \frac{Fl^2\tau_s}{1 + Fl^2\tau_s} \quad \text{and } q_s = 1 - p_s \frac{1 - p_{s+1}}{q_{s+1}}, \tag{4}$$

where τ_s denotes the waiting time for emission of one of the s atoms of a cluster onto the adjacent terrace. The upper cutoff i^* of the product denotes a cluster size above which all islands can be regarded as stable. The continued fraction q_s is anchored at $s = i^*$ with $q_{i^*} = 1$. Desorption of adatoms has been neglected.

The right hand side of (3) is obtained by the following reasoning: First one identifies the nucleation rate with $D\rho_1\rho_{i^*}$, i.e., with the rate at which a critical island captures an adatom [12]. The adatom density is assumed to vary slowly, so that $F \approx \rho_1 D/l^2$, because the deposition rate must be balanced by the rate at which adatoms vanish forever by being bound to a stable island. The latter event requires diffusion over the typical distance l. The

 0031-9007/95/74(11)/2062(4)$06.00

nucleation rate is thus $(F^2/D)l^4\rho_{i^*}/\rho_1$. Using the solution $\rho_s/\rho_{s-1} = p_s/q_s$ of the rate equations

$$d\rho_s/dt = D\rho_1\rho_{s-1} - D\rho_1\rho_s - \rho_s/\tau_s + \rho_{s+1}/\tau_{s+1} \tag{5}$$

for $2 \le s \le i^*$, assuming $d\rho_s/dt \approx 0$, gives (3).

If $1 \gg p_s \approx Fl^2\tau_s$ for all $s \le i^*$, i^* is the critical cluster size. Then all q_s can be replaced by 1, and (3) can be solved for l, leading to (1) with [4,5,10]

$$\gamma(i^*) = \frac{i^*}{2i^* + 2 + d_f}. \tag{6}$$

The condition $p_s \ll 1$ is often violated. An island is called stable if $Fl^2 \gg 1/\tau_s$, so that p_s is practically 1. Hence stability depends on the deposition rate F, whereas i^* is in general only an upper bound for unstable cluster sizes. Moreover, one finds [9] that the stability of islands does not vary monotonously with their size. Certain values of s allow particularly stable cluster structures, so-called "magic islands." An example are heptamers on Pt(111) where six atoms are grouped around a central one on a triangular lattice, so that every atom has at least three lateral neighbors. Adding one more atom gives a much less stable cluster, as this atom can at most have two lateral neighbors. Also the smaller clusters are much less stable than the heptamer. This shows that the factors p_s may be close to 1 for the magic numbers $s^* = 7$, $s^* = 10$, etc. while those for 1–6 and in between the magic numbers are $\ll 1$. Then (6) is no longer true. Instead, $\gamma(i^*)$ has to be replaced by $\gamma(i_0^*)$, where $i_0^* + 1$ is the size of *the smallest stable island.* This result is obtained by applying the identity $q_s + p_s - 1 = (q_{s+1} + p_{s+1} - 1)p_s/q_{s+1}$ to show that the product over all q_s with $s > i_0^*$ equals the one of the corresponding p_s's.

In order to check these predictions we developed a new algorithm for simulating MBE. The basic idea is a coarse graining of the lattice parallel to the layers. Growth starts with a flat substrate, the surface of which is divided into a square lattice of L^2 cells of $(\Delta x)^2 > i^*$ atomic sites each. At later times the surface of the growing film remains divided into L^2 cells, but they may vary in height. The surface configuration is characterized by the number of completed layers $h(j)$ below cell j, a partial filling of this cell with $0 \le m(j) < (\Delta x)^2$ atoms, and a step indicator $is(j) = 1$ or 0 depending on whether or not the cell contains the edge of an island larger than i^*.

The implementation of the growth kinetics will first be described in the absence of magic islands. Then all cells with $1 \le m(j) \le i^*$ can lose up to $m(j)$ atoms to neighboring cells by diffusion. For simplicity we assume a single time constant $t_D = (\Delta x)^2/D$ for all these processes. It corresponds to the time step of the simulation. As soon as more than i^* atoms are gathered in the same cell j they are supposed to form a stable island within one time step: $is(j)$ is set 1 indicating that the cell has changed from a possible source of diffusing atoms into a perfect sink. It is assumed that any adatom coming closer to the island edge than Δx is incorporated into the growing film within time t_D. Deposition of an atom means incrementing $m(j)$ by 1 for a randomly chosen cell j. This may happen in any simulation step with a probability that guarantees the correct average waiting time $1/[FL^2(\Delta x)^2]$ between deposition events. If an atom is deposited into a cell with an island edge, it is assumed to be incorporated within the same time step, which is long enough to allow diffusion over a distance Δx; no distinction is made between deposition close to a downward or to an upward step, i.e., step edge barriers are neglected here. When $m(j) \ge (\Delta x)^2$ the local number of complete layers $h(j)$ is incremented by 1, $m(j)$ is reduced by $(\Delta x)^2$, and the step indicator is updated such that the island edge invades the neighboring cells of lower height.

A few remarks on the applicability of the algorithm are in order: Only one island per cell is allowed by the algorithm. This requires $\Delta x \ll l$. As l results from the growth kinetics, this is a consistency check for the simulation. The minimum arm width for fractal islands is given by the coarse graining length, so that Δx can be identified with the diffusion length along the island edge [13]. Taking the existence of magic islands into account is straight forward. Here we consider only the case where islands of sizes s^* and all $s > i^* > s^*$ are stable. Once the cell contains a number of atoms $m(j)$ in the stability gap this number cannot decrease below s^* anymore. Further details of the algorithm can be found in Ref. [14].

Coarse graining has several benefits: Computation time is reduced by a factor $(\Delta x)^{-2}$, and we do not have to implement edge diffusion explicitly; edge instabilities can only occur on distances larger than Δx. A major advantage of this algorithm is that any i^* and s^* can easily be implemented without the need of an underlying lattice symmetry which would make the values microscopically plausible. Therefore the theoretical prediction (6) can be checked by computer simulation even for values i^* and magic island sizes which are not accessible in laboratory experiments. In contrast to all previous MBE simulations diffusion is performed with parallel rather than random sequential updating. The coarse graining is very similar to noise reduction algorithms [15]. There the counters can only increase.

The island density at fixed coverage $\theta = 0.12$ is plotted in Fig. 1 for $i^* = 1, \ldots, 4$. Obviously increasing i^* leads to larger island sizes since the density decreases by nearly 1 order of magnitude, as predicted by (6) and seen in STM experiments [1]. The value for $i^* = 1$ and $D/F = 10^8$ is in quantitative agreement with the one obtained in essentially the same model without coarse graining and with random sequential updating [16]. The exponents $\gamma(i^*)$ obtained from this plot are summarized in Table I along with the ones predicted by (6) with $d_f = 1.7$

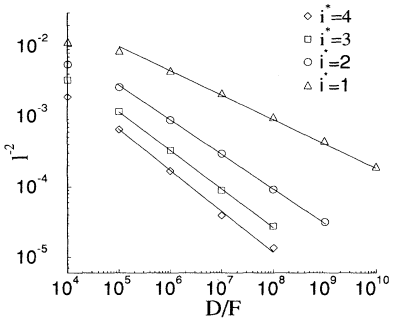

FIG. 1. Island density for various critical sizes i^*.

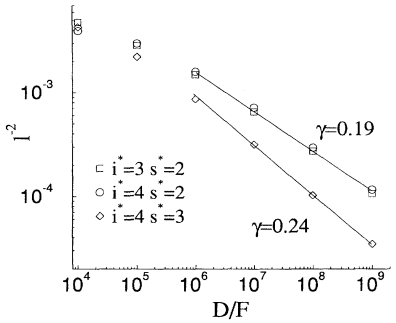

FIG. 2. Density of islands with $s > i^*$ for $i^* = 3, 4$ and $s^* = 2, 3$.

[16,17]. Similar values have been obtained independently by Amar and Family [8]. We also measured the adatom density

$$\rho_1 \approx Fl^2/D \equiv l_1^{-2}. \quad (7)$$

The values of $\gamma(i^*)$ obtained this way are also given in Table I. It will be shown below that finite size effects are responsible for the difference between the measured exponents for $i^* = 1$ and 4. Apart from $\gamma(1)$ all measured exponents are somewhat smaller than the predicted ones. Ratsch *et al.* [18] proposed to invert (6) for continuous i^* to interpret the data in terms of effective critical island sizes. We find that the effective i^* is at least 15% smaller than the integer value used in the simulation.

Figure 2 shows the corresponding results for $i^* = 3, 4$ in the presence of a magic island of size $s^* = 2$ or 3. As predicted only the value of s^* determines γ. Although the measured exponent 0.19 is slightly larger than the expected value $\gamma(1) \approx 0.17$, it still can be taken as signature of the smallest stable islands having size $s^* = 2$. For $s^* = 3$ and $i^* = 4$ the exponent $\gamma = 0.24$ is in perfect agreement with the expected value $\gamma(2)$.

The scaling functions $f(x)$ for several values of i^* with and without a magic island size $s^* = 2$ are shown in Fig. 3. All islands of the same or larger size than the smallest stable island have been counted. Without the magic island a good data collapse is obtained for D/F between 10^7 and 10^9, coverages θ between 0.05 and 0.25, and coarse graining lengths Δx (or arm widths of the fractal islands) between $\sqrt{2}$ and 4, confirming (2). The distribution functions are sharply peaked around $s/\bar{s} = 1$ and become narrower with increasing i^*. This is in agreement with results obtained for different models [8,18,19] and experiments [1]. Our scaling functions are narrower than those of Refs. [1,8,16,18,19], but wider than the ones obtained from rate equations [7]. The coarse graining is not the reason for this difference, as our results hardly depend on Δx. Possibly the diffusion length of individual adatoms fluctuates less for parallel updating than for random sequential updating. It is conceivable that this reduces the scattering of the island sizes around their average size.

TABLE I. Predicted and measured exponents $\gamma(i^*)$.

i^*		1	2	3	4
$\gamma(i^*)$	Eq. (6)	0.175	0.26	0.31	0.34
	Fig. 1	0.172	0.24	0.275	0.29
	(ρ_1)	0.2	0.22	0.24	0.32

In the presence of magic islands there is no data collapse for different coverages anymore as demonstrated in Fig. 3. The cluster size distributions for three coverages ($\theta = 0.05$, 0.1, and 0.15) are shown for $D/F = 10^8$ and $s^* = 2$, $i^* = 3$. The distributions clearly become sharper with increasing coverage. No dependence on i^* could be observed for fixed s^*. Absence of scaling is not so surprising in view of the high population of immobile and stable dimers ($s = 2$) on the surface. They are collected by the growing islands hence providing a second mechanism for the increase of $\bar{s}$ with θ, independent of adatom diffusion over a unique characteristic distance l.

It is reasonable to assume that similar results hold for all magic islands. Recently Zuo *et al.* [3] used diffraction experiments to measure $l(F)$ for Cu(100). They found that γ changes from about 1/6 for a temperature of 223 K to about 3/10 for 263 K and concluded that the critical island size jumps from $i^* = 1$ to $i^* = 3$. However, their

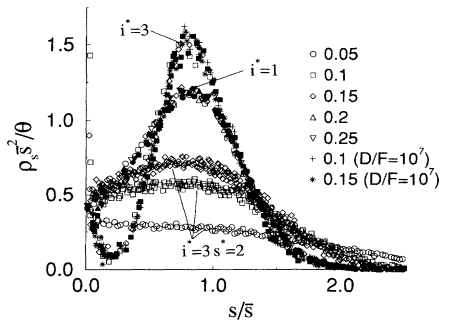

FIG. 3. Scaling function $f(x)$ [Eq. (2)] for different critical cluster sizes $i^* = 1, 3$, the latter with and without a magic island $s^* = 2$. Filled (open) symbols, $D/F = 10^9$ (10^8).

ab initio calculations show that pentamers are less stable than trimers. Therefore i^* in the sense of an upper bound for unstable sizes [4,5] is larger than 3. Our results explain their measured exponent, because it is determined by the smallest stable island size $s^* = 4$ rather than by i^*. Moreover, we predict that for 263 K (2) is violated.

Finally we briefly address finite size effects. Three lengths have to be compared with the system size $L\Delta x$. The first one is the typical distance l between islands and the second is the typical distance l_1 between adatoms, as defined in (7). The third length, $l_0 = (D/F)^{1/4}$, is the only one which has the right dimension without invoking the lattice constant a. l_0 is the average distance an adatom travels before the deposition of the next atom, if there are neither island edges nor other adatoms encountered. For $L\Delta x < \max(l_0, l)$ and periodic boundary conditions the system, therefore, contains only one island [20]. Similarly, vincinal surfaces with a terrace width smaller than $\max(l_0, l)$ should grow in step flow mode. For simplicity we assume $d_f = 2$ in the following discussion. Then it follows from (6) and (7) that $l \ll l_0 \ll l_1$ for $i^* < 2$, while all inequalities are reversed for $i^* > 2$. For $i^* = 2$ all three lengths are equal. This shows that for $i^* = 1$ the adatom density is more susceptible to finite size modifications than the island density and explains why the value of γ obtained from Fig. 1 is more reliable than the one obtained from ρ_1 as shown in Table I. For $i^* > 2$ the opposite is true. We believe that this is the reason why for $i^* = 4$ we find island densities which tend to be too large, leading to an underestimation of the exponent γ. Figure 4 shows the size dependent island and adatom densities for $i^* = 1$ and $D/F = 10^{10}$. For $L\Delta x < l_0 \approx 300$ the island density decreases as there is essentially one island in the system. For larger systems the island density increases again and approaches its asymptotic value $(F/D)^{2\gamma}$. The adatom density reaches its asymptotic value $(F/D)^{1-2\gamma}$ only much later, for $L\Delta x > l_1 \approx 2000$.

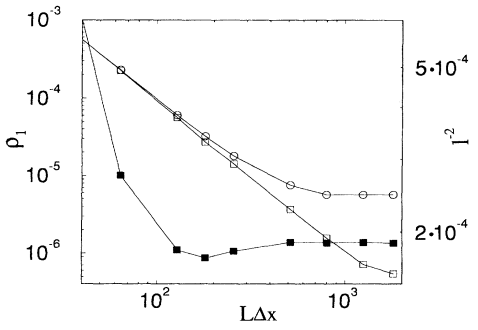

FIG. 4. Finite size behavior of the island (filled) and adatom (empty) density for $i^* = 1$. Circles, $D/F = 10^7$; squares, $D/F = 10^{10}$.

We thank S. Bales, J. Evans, F. Family, D. Vvedensky, and A. Zangwill for communicating their results prior to publication and the GMD for providing us with computer time on their CM5. This work was supported by the Deutsche Forschungsgemeinschaft through SFB 166.

*Present address: HLRZ c/o Forschungszentrum Jülich, D-52425 Jülich, Germany.

[1] J. A. Stroscio and D. T. Pierce, Phys. Rev. B **49**, 8522 (1994).
[2] Y. W. Mo, J. Kleiner, M. B. Webb, and M. Lagally, Phys. Rev. Lett. **66**, 1998 (1991).
[3] J.-K. Zou, J. F. Wendelken, H. Dürr, and C.-L. Liu, Phys. Rev. Lett. **72**, 3064 (1994).
[4] J. A. Venables, G. D. Spiller, and M. Hanbücken, Rep. Prog. Phys. **47**, 399 (1984).
[5] S. Stoyanov and D. Kashchiev, in *Current Topics in Material Science,* edited by E. Kaldis (North-Holland, Amsterdam, 1981), Vol. 7.
[6] M. C. Bartelt and J. W. Evans, Phys. Rev. B **46**, 12675 (1992).
[7] G. S. Bales and D. C. Chrzan, Phys. Rev. B **50**, 6057 (1994).
[8] J. G. Amar and F. Family, following Letter, Phys. Rev. Lett. **74**, 2066 (1995).
[9] G. Rosenfeld, A. F. Becker, B. Poelsema, L. K. Verheij, and G. Comsa, Phys. Rev. Lett. **69**, 917 (1992).
[10] J. Villain, A. Pimpinelli, and D. E. Wolf, Comments Cond. Mat. Phys. **16**, 1 (1992).
[11] J. Villain, A. Pimpinelli, L.-H. Tang, and D. E. Wolf, J. Phys. I (France) **2**, 2107 (1992).
[12] For logarithmic corrections neglected here, see L. H. Tang, J. Phys. I **3**, 935 (1993).
[13] A. Pimpinelli, J. Villain, and D. E. Wolf, J. Phys. I (France) **3**, 447 (1993).
[14] D. E. Wolf, in *Scale Invariance, Interfaces, and Non-Equilibrium Dynamics,* edited by M. Droz *et al.* (Plenum, New York, 1995).
[15] J. Kertész and T. Vicsek, J. Phys. A **19**, L257 (1986).
[16] J. G. Amar, P. M. Lam, and F. Family, Phys. Rev. B **50**, 8781 (1994).
[17] R. Q. Hwang, J. Schröder, C. Günther, and R. J. Behm, Phys. Rev. Lett. **67**, 3279 (1991).
[18] C. Ratsch, A. Zangwill, P. Šmilauer, and D. D. Vvedensky, Phys. Rev. Lett. **72**, 3194 (1994).
[19] M. C. Bartelt and J. W. Evans, J. Vac. Sci. Technol. A (to be published).
[20] P. Jensen, A.-L. Barabási, H. Larralde, S. Havlin, and H. E. Stanley, Phys. Rev. E **50**, 618 (1994).